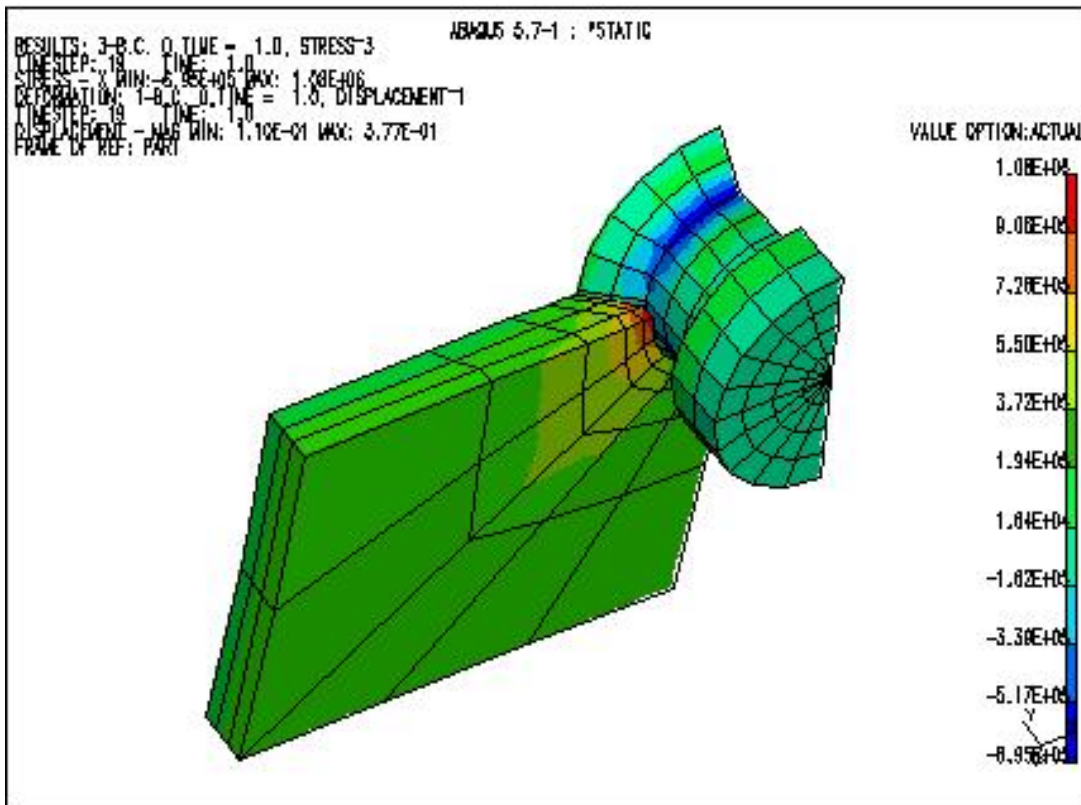


Geng-Sheng Wang

Computational Method for Evaluating the Fatigue Life of Mechanical Joints



Presentation at the 21st Symposium
ICAF' 2001
International Committee on Aeronautical Fatigue
Centre de Congrès Pierre Baudis
Toulouse, France
June 25-29, 2001

SWEDISH DEFENCE RESEARCH AGENCY

Aeronautics Division
SE-172 90 Stockholm

FOI-R--0096--SE

May 2001

ISSN 1650-1942

Scientific report

Computational Method for Evaluating the Fatigue Life of Mechanical Joints

Geng-Sheng Wang

Issuing organization FOI – Swedish Defence Research Agency Aeronautics Institute SE-172 90 Stockholm	Report number, ISRN FOI-R--0096--SE	Report type Scientific report
	Research area code 1. Defence Research	
	Month year May 2001	Project no. E824577,E824578
	Customers code 3. Aeronautical Research	
	Sub area code 11 Defence Research for the Government	
Author/s (editor/s) GengSheng Wang	Project manager GengSheng Wang	
	Approved by	
	Scientifically and technically responsible	
Report title Computational Method for Evaluating the Fatigue Life of Mechanical Joints		
Abstract (not more than 200 words) <p>Difficulty in the fatigue design of fastener is due to contact, friction, plasticity, fretting, wear and tear, etc. Combination of these factors often excludes the use of analytical methods. This paper shows that strategies may be determined nowadays based on the modern computational techniques and the advanced crack growth models to analyse fatigue crack initiation and propagation even when friction, contact, interference fitting, fretting, and plasticity are involved. With a probabilistic solution, effects of multiple site damage and environmental attacks may also be addressed for various joints using conventional as well as advanced fastener systems.</p>		
Keywords fatigue, mechanical joints, probability, multiple site damage, corrosion		
Further bibliographic information	Language English	
ISSN 1650-1942	Pages 29 p.	
	Price acc. to pricelist Security classification	

Totalförsvarets Forskningsinstitut - FOI Aeronautics Institute 172 90 Stockholm	Rapportnummer, ISRN FOI-R--0096--SE	Klassificering Vetenskaplig rapport
	Forskningsområde	
	Månad, år Maj 2001	Projektnummer E824577,E824578
	Verksamhetsgren 3. Flygteknisk forskning	
	Delområde 11 Försvarsforskning för regeringens behov	
Författare/redaktör GengSheng Wang	Projektledare GengSheng Wang	
	Godkänd av	
	Tekniskt och/eller vetenskapligt ansvarig	
Rapportens titel (i översättning) Computational Method for Evaluating the Fatigue Life of Mechanical Joints		
Sammanfattning (högst 200 ord) <p>Difficulty in the fatigue design of fastener is due to contact, friction, plasticity, fretting, wear and tear, etc. Combination of these factors often excludes the use of analytical methods. This paper shows that strategies may be determined nowadays based on the modern computational techniques and the advanced crack growth models to analyse fatigue crack initiation and propagation even when friction, contact, interference fitting, fretting, and plasticity are involved. With a probabilistic solution, effects of multiple site damage and environmental attacks may also be addressed for various joints using conventional as well as advanced fastener systems.</p>		
Nyckelord fatigue, mechanical joints, probability, multiple site damage, corrosion		
Övriga bibliografiska uppgifter		Språk English
ISSN 1650-1942		Antal sidor: 29 s.
Distribution enligt missiv		Pris: Enligt prislista Sekretess

COMPUTATIONAL METHOD FOR EVALUATING THE FATIGUE LIFE OF MECHANICAL JOINTS

* G. S. Wang

Abstract

Fasteners are among the most fatigue critical details in aircraft design due to their high stress concentration. Empirically, multiple parameters involved in the fastener design require extensive fatigue tests that often prolong the product development cycle, and increase the cost. Omission of fatigue tests may occur for potentially fatigue critical parameters during the development stage due to the cost and time schedule, leaving either heavy structures or fatigue weak points that need costly remedy. Difficulty in the fatigue design of fastener is due to contact, friction, plasticity, fretting, wear and tear, etc. Combination of these factors often excludes the use of analytical methods. This paper shows that strategies may be determined nowadays based on the modern computational techniques and the advanced crack growth models to analyse fatigue crack initiation and propagation even when friction, contact, interference fitting, fretting, and plasticity are involved. With a probabilistic solution, effects of multiple site damage and environmental attacks may also be addressed for various joints using conventional as well as advanced fastener systems.

Introduction

Due to complicated interactions among friction, contact, interference fitting, clamping force, surface condition, and different materials in sheets and fasteners, analyses of fatigue life at mechanically fastened joints are often a challenge. The multiple parameters involved in the fastener design lead to uncertainty in fatigue life whenever any parameter is changed. More than often, fatigue tests have shown that fatigue lives can be significantly different if fastener parameters are changed even though the same materials and type of joint are considered. Enormous number of fatigue tests is required if the fatigue life can only be empirically determined, especially when the effect of fastener parameters is to be identified.

Based on some success in applying fracture mechanics methods to analyse the fatigue life of mechanical joints, this paper will introduce a new analytical framework to predict fatigue life at fastener joints. The method is based on modern computational mechanics. The finite element method involving contact, friction, interference fitting, pre-tension, and a non-linear geometrical and material model is used to identify stress severity at fastener joints. Together with modelling of fretting fatigue crack initiation mechanisms, small crack growth behaviour, and load interaction, a systematic method to identify crack initiation locations, to analyse

* Aeronautical Research Institute, The Swedish Defence Research Agency
SE-172 90 Stockholm, Sweden, tel: +46-8-555 04 488, fax: +46-8-25 89 19, email
wgs@foi.se

crack initiation and propagation etc is developed. With a limited number of experimental fatigue tests for one type of mechanical joint to calibrate the model, it is demonstrated that the analytical model is capable of dealing with fatigue life prediction of different types of joints and fastener systems.

Since the model is capable of evaluating the fatigue damage initiated at material defects and initial surface damages, the probabilistic model presented at the previous ICAF conference is extended to analyse the probability of crack initiation and propagation. As a result, important issues like production quality, material inhomogeneity, initial defects in material and on the contact surface, and interface conditions can be analysed such that a much more realistic scenario of multiple site damage is evaluated for the mechanically fastened joints. Using the model it is possible to simulate how the choice of material, production quality, and the severity of usage may affect multiple site damage initiation. Furthermore, environmental impact on the multiple site damage is also addressed based on the pitting crack initiation mechanism and the environmental assisted crack growth acceleration.

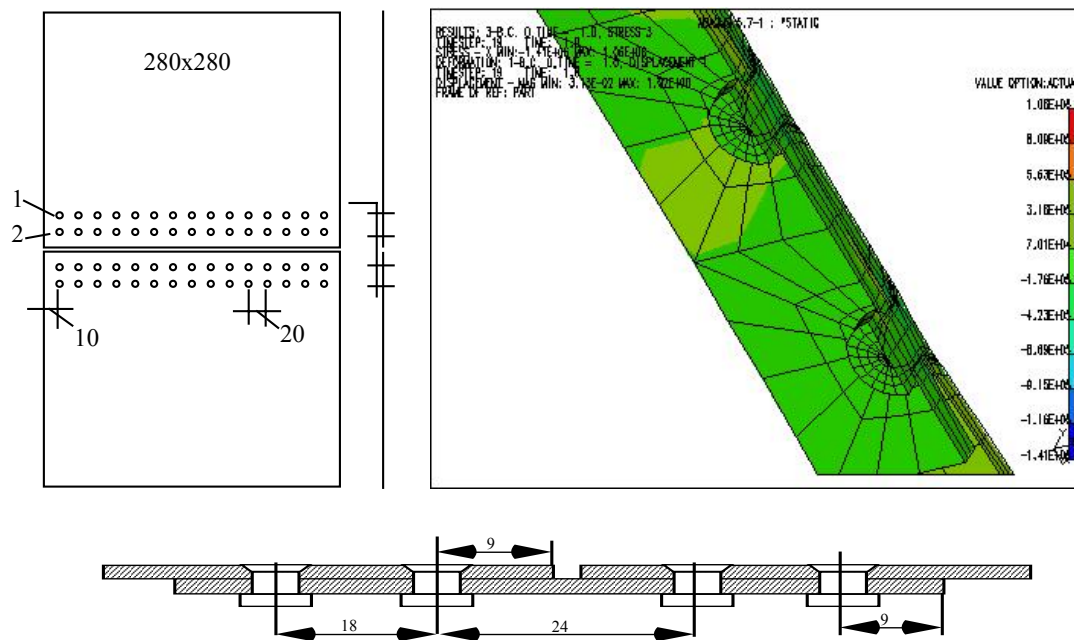


Fig.1: The lap-joint fastener specimen for the multiple site damage fatigue test, and the finite element model of the specimen.

Stress Severity

To highlight the complicated stress condition at the mechanical joints, a detailed stress analysis was performed for a lap joint multiple site damage fatigue test panel as shown on the left side of Fig.1. This specimen was used in a co-operation program performed within a

BRITE-EURAM project concerning the characteristics of multiple site damage problems in ageing aircraft (Gattaneo, *et al*, ref.¹). The specimen was designed to represent the butt joints between upper and lower shell of the front fuselage of a civil aircraft. For this specimen, countersink fasteners are manufactured according to the factory standard.

Various three-dimensional finite element models were created as shown for an example on the right side of Fig.3. Linear solid elements are used in the finite element models with the smallest elements close to the highest possible stress locations. The linear elements are chosen due to their good convergence for non-linear analyses. All the possible contact surfaces are modelled according to a friction contact model (Coulomb friction model) available in a commercial code (ABAQUS ref.²). A “neat fit” condition is model between the fastener, the hole, and the sheets since the conventional rivets with negligible interference and clamping force were used for the specimen. The initial residual stresses around the hole are not considered.

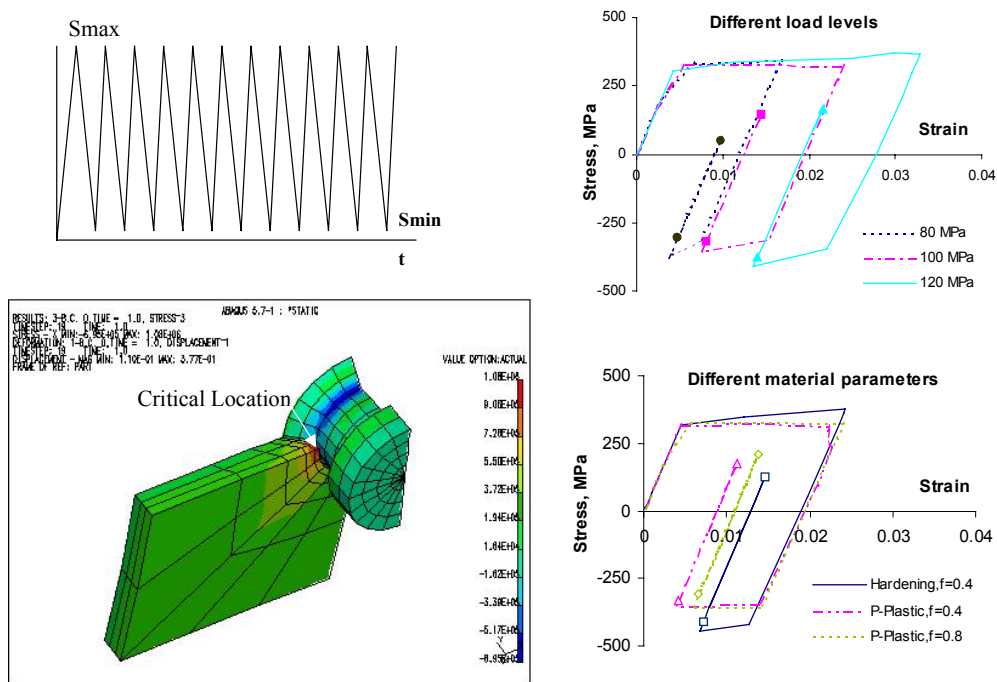


Fig.2: Stress responses at the critical location for various load levels and material parameters under fatigue loading.

The stress analysis was initially performed when only friction and contact are considered. The material was assumed to be linear. The stress analysis showed an excellent agreement between the stress concentration locations and the experimental fatigue crack initiation locations. A very high stress concentration was computed with a concentration factor as high as $K_t = 10.8$, indicating that plastic yield could occur at a much lower load level (31MPa) for the panel made of the aluminium alloy with a yield stress of 332MPa . The finite element analyses also showed that the out-of-plane deformation was severe, indicating that geometrical non-linear deformation should also be considered.

Refined analyses were performed when non-linear geometrical deformation, plastic yield, and cyclic strain hardening were included. The analyses were performed for a cyclic fatigue loading condition with a maximum level of 100MPa and a stress ratio of $R = 0.1$. Fig.2 shows some stress-strain results under the cyclic loading at the highest stress concentration location (side of the hole on the contact surface between sheets, see Fig.2).

The stress analyses indicated that even though plastic deformation is severe under a fatigue loading condition, the subsequent stress range and concentration are not as severe, see the right side of Fig.2. There is a large difference in the material response between the first few fatigue cycles and the subsequent cycles. Similar stress-strain responses appear for various friction and material assumptions, see the lower right of Fig.2. An early plastic deformation results in a total strain of more than 2 % under an elastic perfectly plastic assumption and a coefficient of friction of 0.8. The range of stress is slightly more than twice of the yield stress for the first load cycle with a stress ratio around $R = -1$ (compared to the fatigue stress ratio of $R = 0.1$). Reverse yield occurs for the first fatigue cycle with a strain range as high as one third of the total strain.

Under the subsequent fatigue cycles, an elastic shakedown is established. The stress-strain is stabilised linearly. The shakedown seems to be due to residual stresses created by both the plastic yield and the friction between the hole, the fastener, and the plate. The stress can be reached only at a level less than two third of the stress for the first load cycle. The stress ratio is stabilised at a value of about $R = -2.4$. The stress concentration is reduced to 1.45 from the linear value of 10.8. The concentration of stress with respect to the stress range becomes 5.6.

In all the stress analyses, a constant coefficient of friction is assumed between all the possible contact areas to facilitate finite element analyses. The friction is a complex issue since the coefficient of friction may be different at different locations and fatigue cycles. The constant friction assumption is to obtain an average information without involving too much computational difficulty. The assumption allows analyses of friction in different average conditions. For various coefficients of friction, for example, some results are presented in Fig.2. The trend shows that reduction in the coefficient of friction will reduce residual strain and increase stress concentration at the shakedown condition.

Apparently, the large plastic yield leaves no linear correlation between load and local stress. For the same stress ratio, three fatigue load levels were analysed; 80MPa , 100MPa , and 120MPa . These levels cover the loading conditions used in fatigue tests for the lap joint panel. In these analyses, the coefficient of friction is chosen to be 0.4, and strain hardening is considered. The computational stress-strain at the critical location is shown on the upper right side of Fig.2. There is very large plastic deformation at the load of 120MPa . The total strain is more than 3 % for the first peak load. At the first minimum load, the residual strain remains to be more than 1%. It is interesting to find that the stress-strain response can still be stabilised for the subsequent fatigue cycles similar to those at lower fatigue load levels. In the stabilised shakedown condition, the stress-strain response appears to be linear. There is no further cyclic plastic yielding after the joint has been “stabilised”.

There is a similar stress-strain response for the load as low as 80MPa . Still, there is a substantial plastic yield for the first load cycle. The total strain is larger than 1 % at the first load cycle. At the stabilised state, the strain is slightly less than 1%. The low stress level seems to cause less residual stress, and the reverse yield occurs later.

These stress analyses show that there is substantial non-linearity at fastener joints even if the nominal stress is low. The excessive plastic yield may reduce the effect of initial residual stresses and rationalise the omission of initial residual stresses in the finite element model. The analyses also showed that it is possible and affordable to apply finite element analyses based on commercial codes when friction, contact, and non-linearity are considered. The extraordinary feature in the stress at the joints is that an elastic shakedown stress-strain state may be created under fatigue loading at the critical location even at a rather high fatigue load level. This feature may be used to simplify the fatigue analyses of the joints.

Fatigue Crack Growth

A general description of the material response under fatigue loading may be summarised schematically as shown in Fig.3. The stress-strain may be linear as shown in Fig.3 (a) when the stress is less than the yield stress. In this case, fracture mechanics methods may be used to analyse the crack growth according to the theories for both small and long crack growth since the crack growth may be solely determined by the plasticity around the crack tip.

When the stress is high, peak tensile or compressive stress may exceed the yield stress. There will be a gross yield around the stress concentration location. There are two cases to be considered as shown schematically in Fig.3 (b) and (c). If the range of stress is less than that to cause a reverse yielding (e.g. twice the yield stress), a stabilised stress state may be created, as shown in Fig.3 (b). This state is due to the permanent gross yield that creates a system of residual stress to relieve the peak stress concentration. The strain hardening may help to establish the stabilised state since further yield may occur at a higher stress level. In this case, the fracture mechanics methods may still be used so long as the effect of residual stress and its relaxation is properly accounted for.

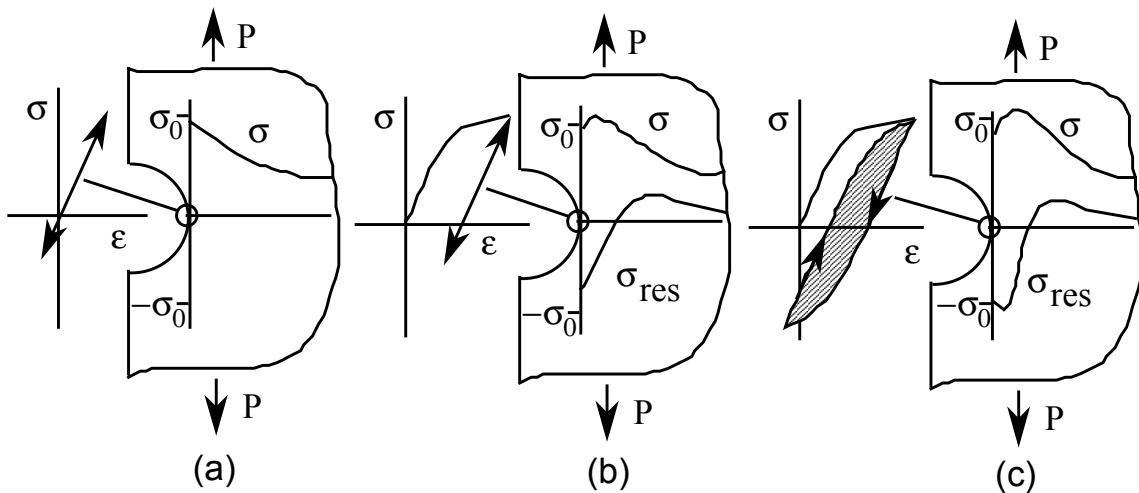


Fig.3: Various models for post yield fatigue problems.

For seldom cases, the material may be subjected to a large deformation-controlled condition due to either high load or low yield stress. A stable cyclic gross reverse yield may occur under fatigue loading as shown schematically in Fig.3 (c). In this case, the fatigue life is no longer solely determined by fatigue crack growth. The metallurgical property of material will affect fatigue damage as well. Fracture mechanics methods can no longer be used alone to deal with the fatigue process since the damage can no longer be determined by the behaviour of the individual crack. One has to consider the gross resistance of material to cyclic plastic

deformation. Other localised methods like the low cycle fatigue models, cyclic material response analyses, and damage mechanics methods etc., may provide ways to deal with the fatigue problems. This case is usually limited to some components operated at extreme temperature with constrained deformation. It often involves short fatigue lives.

The finite element results shown in Fig.2 for the MSD panels under a range of stress levels show that the crack growth in mechanical joints is most probably limited to the problems up to the case as shown in Fig.3 (b). In this case, a stabilised stress-strain linear relation may be established under a fatigue loading condition (in mechanical joints, friction also helps to create further residual stress to reduce the stress severity). Under such a condition, the analysis of fatigue crack growth may be realised using the theories of the fatigue crack growth in a residual stress field.

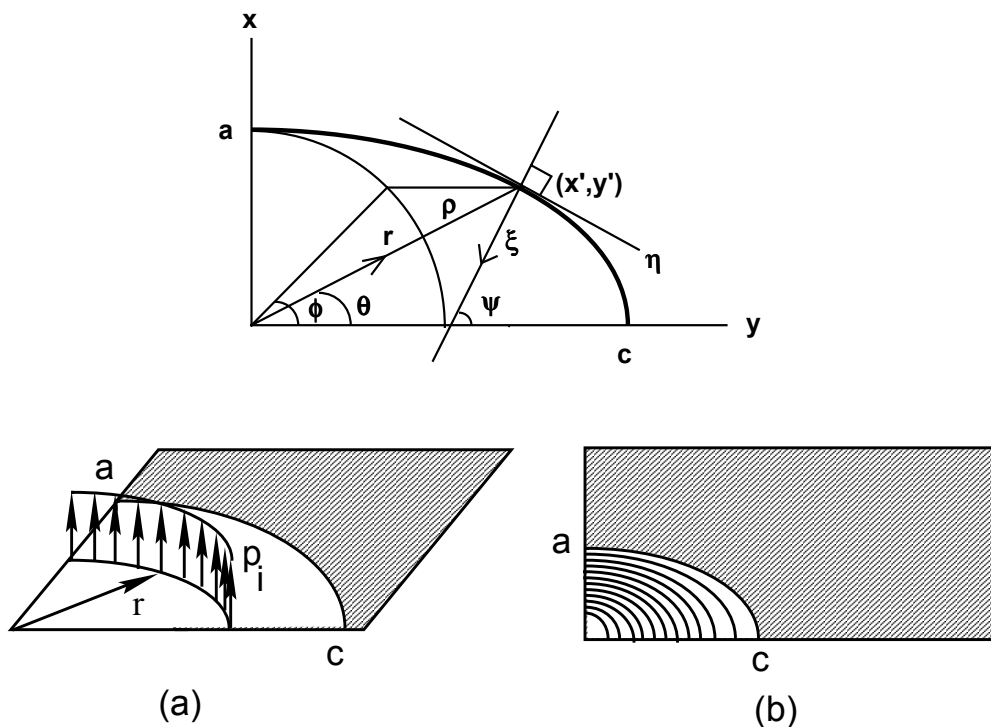


Fig.4. Geometry quantities and arrangement of ring elements for a part-elliptical crack.

Fatigue life is usually divided into crack initiation and propagation stage. The crack initiation may be further divided into crack nucleation and small crack growth stage. The crack nucleation is often referred to the stage that stress risers are created on a smooth surface. This stage is closely related to the early S-N curve fatigue test methods for which smooth small specimens are extensively used. The crack nucleation stage is often not a significant part of fatigue life since various flaws may be pre-existed on the surface due to impurities in material, machine scratches, fretting damages, local plastic yielding, and environmental attacks etc. It is often adequate to consider the crack initiation consists of only the small crack growth phase. If the advanced crack closure models are considered, a total fatigue life analysis may be realised since the model accounts for the small crack growth behaviour as well.

The crack closure model is based on Elber's discovery in the early 70's³, which shows that a fatigue crack could not grow if its tip is not opened. Because of the plastically stretched materials on the crack surface, the irregular crack growth path, and the chemical reactions

occurred around the crack tip due to deformation heat or geometrical concentration of chemicals, the crack tip may remain closed for some part of fatigue loading. The crack closure is especially severe when variable amplitude loading is involved. Peak loads, though they seldom occur, affect significantly the crack closure that may in turn significantly affects the crack growth for the majority of small cycles in a load sequence.

For a part-through crack, the Elber's crack growth relation may be extended using the geometry quantities as shown on the top of Fig.4. The crack growth rate may be expressed as:

$$\frac{d\rho(\theta)}{dN} = f\{\Delta K_{eff}[\rho(\theta)]\} \quad (1)$$

where

$$\Delta K_{eff}[\rho(\theta)] = [\sigma_{max} - \sigma_{op}(\theta)]K^{unit}[\rho(\theta)]. \quad (2)$$

is an effective stress intensity factor range computed for the stress started from the crack opening stress to the peak stress. K^{unit} is the stress intensity factor for a unit load. For a part-elliptical crack, the crack front has values of

$$\rho(\theta) = \begin{cases} a & \text{for } \theta = \pi/2 \\ c & \text{for } \theta = 0 \end{cases} \quad (3)$$

θ is a polar angle and ρ is the polar coordinate of the crack front. In this crack growth relation, the crack growth is defined for the crack front ρ . For example for a surface crack, the crack growth rate in depth may be approximated for $\theta = 90$:

$$\frac{da}{dN} = \frac{1}{w(K_{max})} C [\Delta K_{eff}(a)]^b \quad (4)$$

This relation is an extension of the Paris law when the crack closure and quasi-static effect are considered. In this model, $w(K_{max})$ is a function to account for the effect of the maximum stress intensity factor on the crack growth rate in either the quasi-static growth regime or the near threshold regime. C and b are considered to be material constants. In this model, the key issue is to determine the crack closure so that the crack growth rate can be determined. For many metallic materials, the plasticity is the most dominant crack closure mechanism. If an elastic-plastic solution can be found whenever the crack has propagated into several percent of its own plastic zone, reasonable accurate predictions of crack growth may be realised under a spectrum loading condition.

Finite element methods may be used to evaluate the plasticity induced crack closure. The method is so far not effective and efficient since the analysis involves contact, friction, and plasticity for the cycle-by-cycle crack growth evaluation. An alternative method, the strip yield model has been developed.

The strip yield model assumes that the plastic yield ahead of the crack tip may be approximated in a strip yield manner (Dugdale⁴ and Barenblatt⁵). The linear stress singularity ahead of the crack tip is removed by plastic yield that is approximated as a strip stress acting

in the plastic zone. When a residual stress field is presented, the original Dugdale-Barenblatt strip yield model is extended (Wang, ref.⁶) so that the stress intensity factor at the boundary of the plastic zone should satisfy a condition of:

$$K_L(\rho + r_\rho) + K_{res}(\rho + r_\rho) + K_y(\rho + r_\rho) = 0 \quad (5)$$

In this relation, K_L is the stress intensity factor due to the applied load, K_{res} is the stress intensity factor due to the residual stress, and K_y is the stress intensity factor due to the plastic yield. The model needs linear stress intensity factor solutions for the applied load, the plastic yield, as well as the residual stress field. These stress intensity factors may be determined according to various fracture mechanics theories.

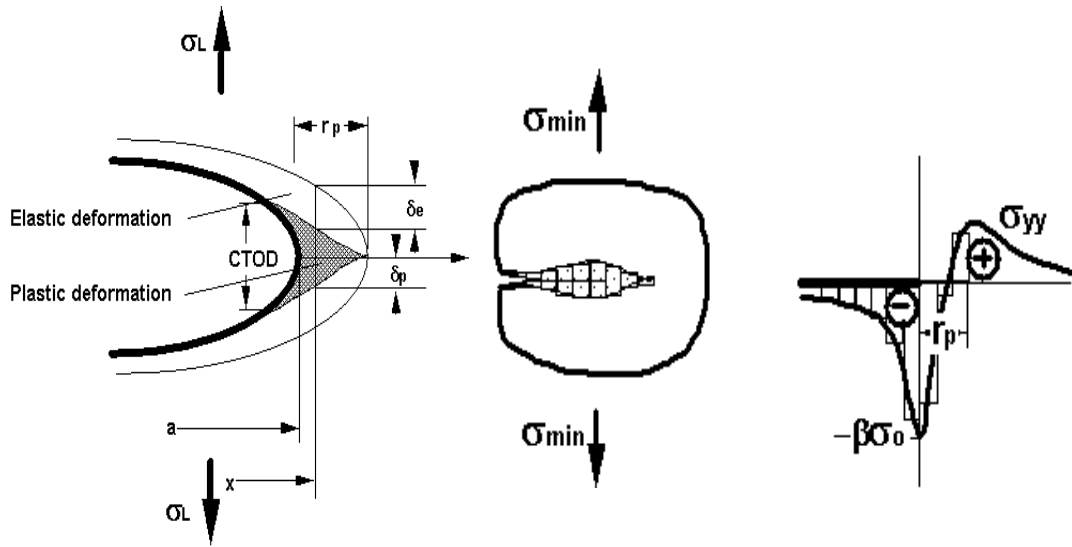


Fig.5: Schematics of the strip yield fatigue crack growth model.

The strip yield model provides not only a solution for the plastic zone size r_p , see Fig.5. When linear solutions can be found for the crack surface displacements, the plastic deformation in the plastic zone can be approximately determined. As shown as the shaded area in the schematic on the left side of Fig.5, the plastic deformation in the plastic zone may be approximated as the gap between an assumed linear elastic crack. The assumed crack is subjected to the yield stress in the plastic zone, with its tip located at the elastic-plastic boundary. This plastic deformation is the “pure” part of plastic stretch. The elastic deformation in the plastic zone is approximated as the linear deformation of the imaginary elastic crack surface. The elastic deformation will be recovered when the applied load, the residual stress, and the strip yield stress are released, see the left side of Fig.5.

The fatigue crack growth can be considered as a process during which the crack tip keeps growing into its own plastic zone with the plastic stretches gradually moved towards the crack surface, see the centre and the left side of Fig.5. Solution of the plastic stretch makes it possible to establish a model (Wang and Blom, ref.⁷) to solve the plasticity induced crack closure by approximating the plastic stretch with a system of small constant stress elements (Dill and Saff⁸, Fuehring and Seeger⁹, and Newman¹⁰). The stress in the plastic zone as well as on the crack surface is numerically determined. The important parameter, the crack opening stress is determined by considering the stress in the element at the crack front.

To simplify the solution for three-dimensional problems, a system of ring elements is established instead of the “bar” elements as for the two-dimensional problems, see Fig.4 (a) (b). The stress on each ring element is assumed to be constant. The assumption is based on the experimental observation of fatigue striations on the surface of part through cracks. The rings cover both the crack surface and the plastic zone with their cross sections along a polar coordinate r axis approximately like the bar element arrangement. On each ring element, the stress is an average of:

$$p_i = \frac{1}{r_{i+1} - r_i} \int_{r_i}^{r_{i+1}} \sigma_{zz}(r) dr \quad (6)$$

The ring elements are assumed to be rigid-perfectly-plastic with the plastic yield on each element determined by:

$$-\beta\sigma_0 \leq p_i \leq \alpha\sigma_0 \quad (7)$$

for the rings in the plastic zone and

$$-\beta\sigma_0 \leq p_i \leq 0 \quad (8)$$

for the rings on the crack surface. Here, α is a coefficient used to account for the average three-dimensional constraint ahead of the crack front. β is a coefficient representing Baushinger's effect. The ring elements act like fatigue striations on the crack surface, resulting in the crack closure under fatigue loading.

In order to solve the stress on each ring, the plastic deformation is solved for the applied load, the residual stress, and the strip yield stress. The deformation on each ring element satisfies a displacement compliance requirement of

$$\delta_p(r, \rho + r_\rho) = \sigma f(r, \rho + r_\rho) + u_{res}(r, \rho + r_\rho) - \sum_{i=1}^n p_i g(r_i, r, \rho + r_\rho) \quad (9)$$

where δ_p is the plastic stretch at a distance r , σf is the crack surface displacement due to the applied stress σ . u_{res} is the crack surface displacement due to the residual stress field, and $p_i g$ is the crack surface displacement due to the yield stress on the ring element i . By solving the linear function system of eq.(9) under the constraints of eq.(7-8), the stress on each ring is determined. The crack opening stress is determined as the load at which the stress at the crack front ring element becomes zero.

When the cyclic plastic yield occurs mainly at the crack tip (the crack tip plasticity dominant condition), this method will have adequate accuracy to deal with crack closure problems. In this solution, stress intensity factors for the residual stress and for the ring elements are required. In addition, analytical solutions of the influence functions for the crack surface displacement due to the applied load, the residual stress, and the unit ring element stress are required. These solutions can be obtained using the approximate three-dimensional weight function theory (Rice¹¹, and Wang¹²). Detailed solution of this model is provided elsewhere (Wang, ref.¹³).

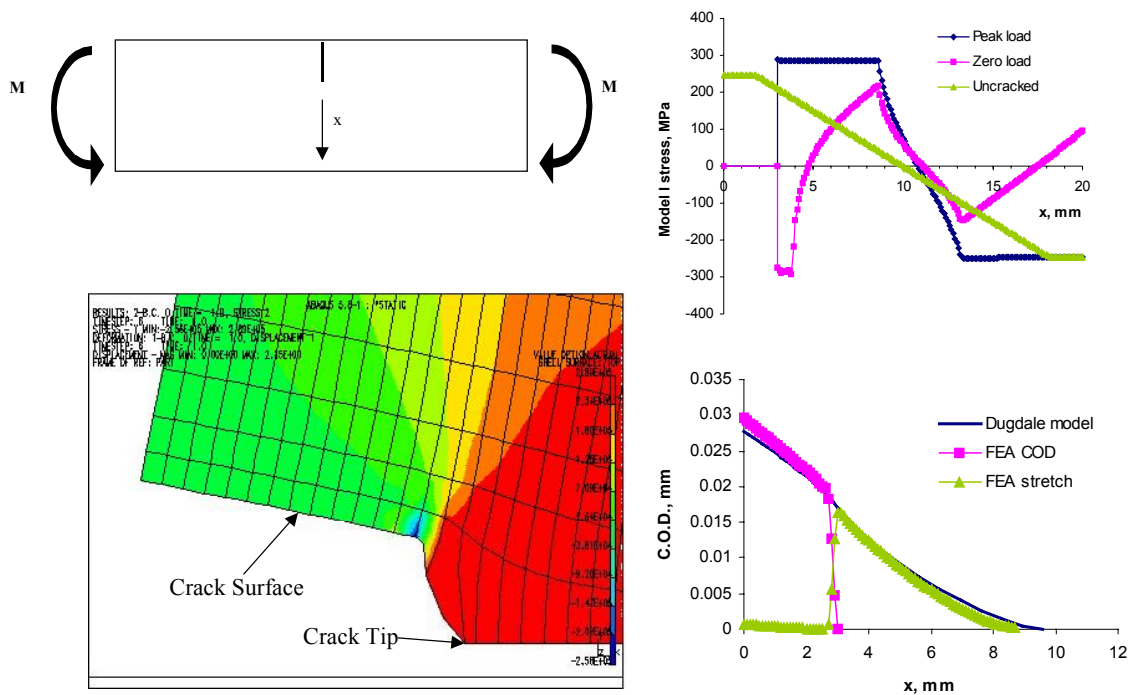


Fig.6: Finite element verification of strip yield model for the post yield problems.

It has been demonstrated that the strip yield model is very effective to account for various aspects of fatigue crack growth behaviour, including the small crack growth problems. Wang (ref.6) has shown that the strip yield model can be used for the fatigue crack growth problems up to a “crack tip plasticity” dominant regime. For the post yield regime, a concern for the evaluation for crack growth in the joints, a verification of strip yield model is shown in Fig.6. A bending specimen with a single edge crack is considered. A high fatigue bending moment is applied to create initial gross yield before the crack is initiated, see the upper right corner of the figure for the stress distribution across the centre section. A crack is then introduced and the plastic deformation at the crack tip is computed based on the finite plasticity model and non-linear geometrical model. Both the plastic zone and the permanent plastic deformation are computed. The finite element results are compared to the strip yield model that is based on the deformation in a residual stress field created by the initial fatigue loading. As shown in the comparison in the lower right of Fig.6, the strip yield model gives very good

approximation for the plastic zone and the permanent plastic deformation. The model can therefore be confidently used for the post-yield crack growth problems when a shakedown stage may be achieved.

For the MSD panels, a mean initial flaw is assumed according to the metallurgical inspection of defects in aluminium alloy (see ref.¹⁴) and some empirical investigations. The initial crack is approximated with a depth of $a_0 = 10\mu\text{m}$ and a size of $c_0 = 20\mu\text{m}$ on the surface at the side of the hole. An intrinsic crack growth rate is determined according to the long crack growth data of aluminium alloy 2024 T3. The crack growth rate is characterised (ref.¹⁵) according to eq.(4) with the material parameters of $b = 3.75$, and $C = 7.68 \times 10^{-11}$. A fracture toughness $K_{cr} = 72.5\text{MPa}\sqrt{\text{m}}$ is calculated using the plain strain and plane stress critical stress intensity factors based on the thickness (1.2 mm). The quasi-static crack growth acceleration is approximated using a function of $w(K_{\max}) = 1 - K_{\max} / K_{cr}$.

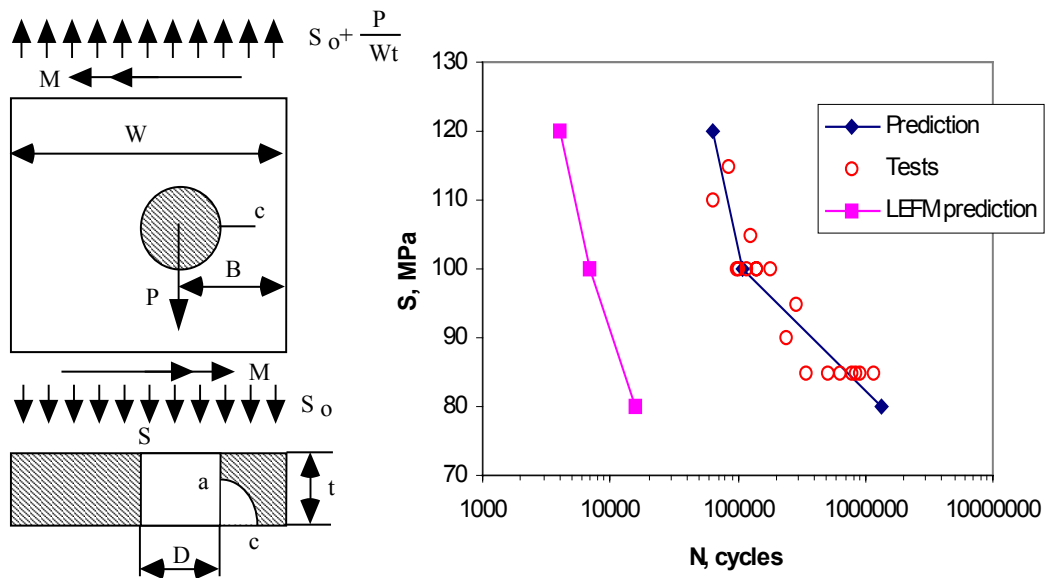


Fig.7: Comparison of computed and test fatigue lives for the MSD test panels.

According to the stress results from finite element analyses, weight functions, influence functions, and the stress intensity factors were determined for both the applied load and the residual stress field. The analyses showed, however, to be non-conservative (with a couple of times longer fatigue lives). The overestimation of fatigue life is considered partly due to the lack of accuracy in the mean rooted average weight function solutions (Wang, ref.13), and the omission of tear and wear in the stress analyses. Unlike the open notch problems in ref.¹⁶, tear and wear should be considered. Fretting, tear and wear intend to reduce the thickness of plate, and to create oxidation debris etc. Such effects are expected to reduce the residual

stress and increase the stress concentration so that the joints will experience a more severe stress condition.

To overcome the shortcoming, a modification is needed in the finite element stress range. When a 15% increase is made for the stress range (from a concentration factor of 5.6 to a value of 6.4), the fatigue lives are reanalysed. A comparison between predictions and test results is shown in Fig.7 with the predictions as lines with solid diamond symbols compared to the experimental results as open symbols. With this modification, the analyses result in a rather satisfactory agreement with the test results for the load ranging from 80MPa up to 120MPa. The analyses are a significant improvement over the linear elastic fracture mechanics (LEFM) solutions shown in the same figure. The LEFM solutions were based on simple forces and bending moments computed from a shell and beam finite element model of the MSD test panel. The forces and bending moments are used to compute fatigue lives in a LEFM model as shown on the left side of Fig.7. The LEFM analyses predicted fatigue lives nearly two orders of magnitude shorter than the test results even though the crack growth model, and the baseline crack growth rate, and the initial crack size are the same.

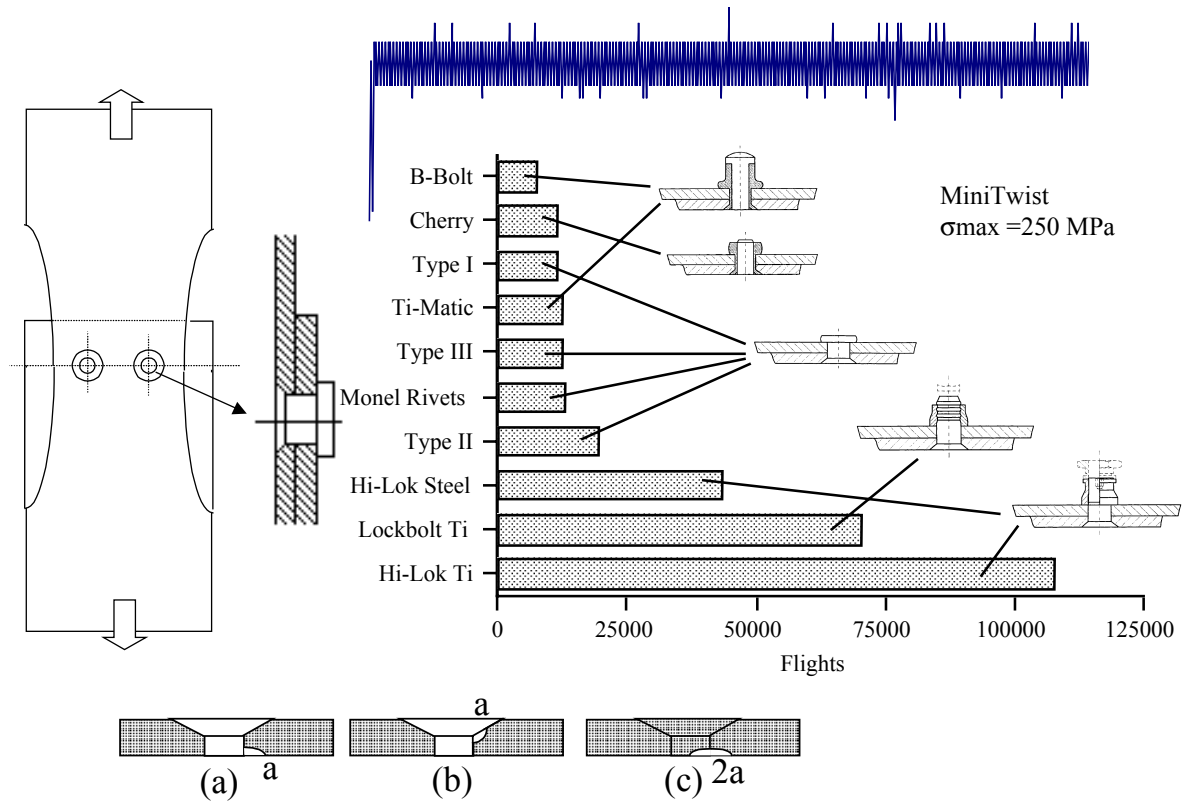


Fig.8: Comparison of fatigue lives for various fastener systems for $\frac{1}{2}$ dogbone specimens.

Joint Types and Fastener Systems

The “neat fitted” is representative for rivet fasteners for which both the clamping force and interference are small. It has yet to be verified whether or not the same knowledge obtained from neat fitted fastener joints can be extended for other types of joints and fastener systems under a spectrum loading condition. There are various fastener systems today that use

interference or heavy clamping force to increase fatigue life. Such fastener systems differ from the rivet system in various ways. For example for the fatigue tests of a so-called $\frac{1}{2}$ dog-bone joint specimen under the mini-TWIST spectrum loading, fatigue lives are significantly different if different fastener systems are used, see the test results as shown in Fig.8.

The fatigue tests showed that the neat fitted fasteners (rivets) gives the shortest fatigue life while the system with heavy clamping force and interference fitting will increase fatigue life (up to one order of magnitude). Fatigue cracks have been observed at the side of the fastener hole, inside of the fastener hole, or away from the hole on the fretting face, see the bottom of Fig.8. As a rule of thumb, cracks initiated inside of the fastener hole give the shortest fatigue life and cracks initiated away from the fastener hole give the longest fatigue life. This phenomenon can be explained by considering an equivalent crack. For the crack initiated inside of the fastener hole, the equivalent crack is the size of crack plus the hole and the countersink. This gives the largest crack and shortest fatigue life. When the crack is initiated at the side of hole, the equivalent crack size equals the size of crack plus the size of hole. This crack is smaller than the crack initiated inside of the hole, and the fatigue is also longer. For the crack initiated away from the fastener hole, the equivalent crack equals the physical crack, resulting in the smallest crack and the longest fatigue life. Generally, rivets with high stiffness (steels) tend to create cracks inside of the hole. The rivets with lower stiffness (titanium alloys) or similar stiffness (aluminium alloys) tends to initiate cracks at the edge of the hole with slightly longer fatigue lives. The biggest gain comes from the interference fitting with high clamping force, from the systems such as the Hi-Lok bolts or the Lockbolts. These systems may give nearly an order of magnitude longer fatigue life since fatigue crack may be initiated away from the hole, resulting in a smaller effective crack and a larger fracture section.

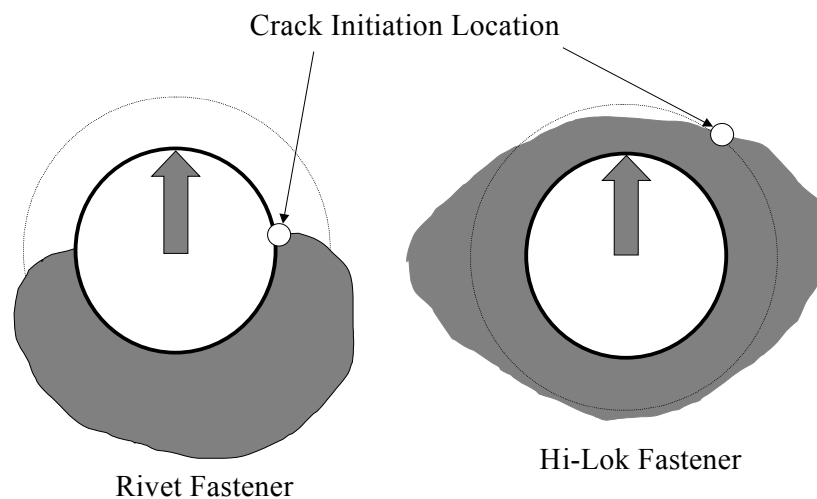


Fig.9: Schematic comparison of the stick-slip boundary at the most frequent fatigue load level for rivet and Hi-Lok fastener in the shakedown condition.

Fretting should be considered along with the stress concentration in order to identify crack initiation locations. Fretting plays an important role in analysing fatigue crack initiation¹⁷, especially if the fretting is close to the stress concentration. For fastener joints, fretting was

frequently observed at the crack initiation locations¹⁸. Fretting is mainly due to a large number of small load cycles occurring at the stress concentration area along the fretting boundary. The stick-slip boundary between the contact surface has been identified¹⁹ to be a major crack initiation location.

The left side of Fig.9 shows a reconstruction of the finite element contact area between the sheet and splice at the shakedown condition for the MSD panel. The stick-slip boundary is determined by checking the relative movement on the opposite sides of the contacted surfaces. The stick-slip boundary for the rivet fasteners is located at the highest stress concentration location (the side of hole in the minimum section). Together with the high stress concentration there, fatigue crack will be initiated much easier at this location.

The analyses of contact and fretting are more useful for the case when fatigue cracks may be initiated at different locations. Similar to the model of the MSD panel, several finite element models were created for different fastener systems for the ½ dogbone specimens. The ½ dogbone specimens are made of the same alloy sheets with a different thickness of 2.5 mm. The hole has a diameter of 5mm, and the half width of the plate is 20mm. The fasteners have a countersink head. This joint has less severe load transfer and secondary bending. Two different fastener systems are considered for this specimen; one for the aluminium rivets, the other for an advanced system of titanium Hi-lok bolts.

In addition to the material difference between aluminium rivets and Hi-lok bolts (Hi-lok bolts are more rigid than aluminium rivets), there is a large pre-tension and some interference for the fitting of the Hi-lok bolts. In the finite element model, this effect is considered by using a shorter-and-thicker-than-the-neat-fit bolt. The dimension of bolt is determined by comparing finite element results to the values from experimental measurements.

The specimens are subjected to a mini-TWIST spectrum as shown at the top of Fig.8. The spectrum is a standard spectrum representing the average wing root load experience of transport aeroplanes. Under this loading condition, plastic yield is different for different load cycles. The shakedown state was analysed by including the maximum and minimum load cycles in the finite element model. Since the mini-TWIST spectrum with a nominal stress of 100 MPa was used in fatigue tests, the maximum stress level of 250MPa and the minimum stress of -58MPa were included in finite element analyses.

Under spectrum loading, the stick-slip boundary changes as a function of the load. Since fretting crack initiation is mainly due to the large number of small load cycles, it is assumed that crack initiation may occur along the stick-slip boundary at the most frequent load level. For the mini-TWIST spectrum, this load level is around the nominal load level.

A reconstruction of the stick-slip boundary from the finite element analyses is shown on the right side of Fig.9 at the most frequent load level for the Hi-lok fasteners. The slick-slip boundary for the rivet fastener is similar to that of the MSD panel as shown on the left side of Fig.9. The frequent crack initiation locations are marked in Fig.9 for both rivet and Hi-lok fasteners. It is remarkable that crack initiation locations are along the stick-slip boundary for both Hi-lok and rivet fasteners. Cracks are mostly initiated about 0.5 mm away from the top of hole for Hi-lok fasteners (around 3 mm from the centre of hole with a diameter of 5 mm) while the cracks are often initiated at the edge of hole for rivet fasteners.

To identify where a fatigue crack may be initiated along the stick-slip boundary, stresses should be considered as well. Fig.10 shows a comparison of the shakedown Mode I stresses

along the broken section of the rivet and Hi-lok fastener joints. Stresses for the rivet fastener are shown on the left side of the figure along a line across the centre of the hole (the broken line). Stress distributions are shown for the Hi-lok fastener along a line 0.5mm above the hole, see Fig.10. The stresses are shown for the peak load and the zero loads. While the peak load shows the stress concentration, the stress at zero gives the result of residual stress distribution.

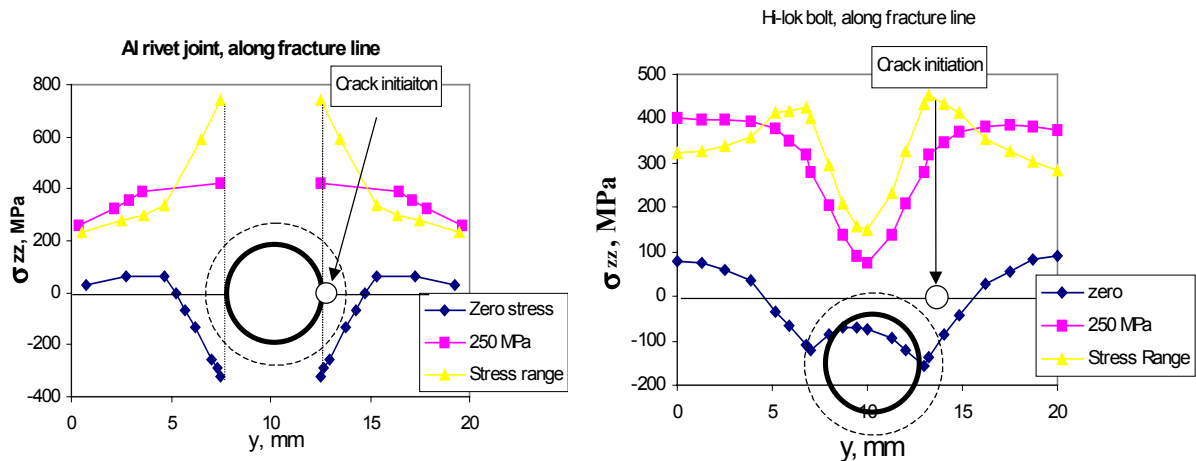


Fig.10: Comparison of stress distributions along the broken lines for both rivet and Hi-Lok fastener.

Even though the crack initiation location may be identified for rivet fasteners along the stick-slip boundary, the peak stress distribution is nearly constant within a considerable area away from the edge of the hole. This stress distribution suggests a possible multiple site crack initiation that is in contradiction to the experimental observation (fractographic observation showed mostly a single dominant crack initiation location). For Hi-lok fasteners, the crack initiation location cannot be identified at all from the peak stress distribution. The stress is actually lower at the crack initiation location, see Fig.10.

In a fatigue process, the range of stress cycles often does more damage than the mean or maximum value. The range of stress is not necessarily related to the maximum stress under an elastic plastic condition since the stress and the load is not linear. The stress ranges for both the rivet and the Hi-lok fastener (between 250MPa to -58 MPa for mini-TWIST spectrum) are calculated and shown in Fig.10 as the curves with triangle symbols.

The distribution of stress range is different from either the maximum stress or the residual stress. The critical areas for the stress range are different. The crack initiation occurs exactly at locations along the slip-stick boundary where there is the highest concentration of the stress range, see the comparison shown in Fig.10. For the rivet fastener, even though the peak stress and slip-stick boundary have revealed an area where crack initiation may occur. This area is relatively large so that it is difficult to determine whether a corner or a surface crack may be initiated close to the edge of the hole. The stress range analyses reveals that a dominant crack will be initiated at the edge of hole where there is the highest stress range concentration. The most direct benefit to consider the stress range is for the Hi-Lok bolts which has lower peak stress at the crack initiation location. The stress range reveals directly where along the stick-skip boundary a fatigue crack may be initiated, see Fig.10.

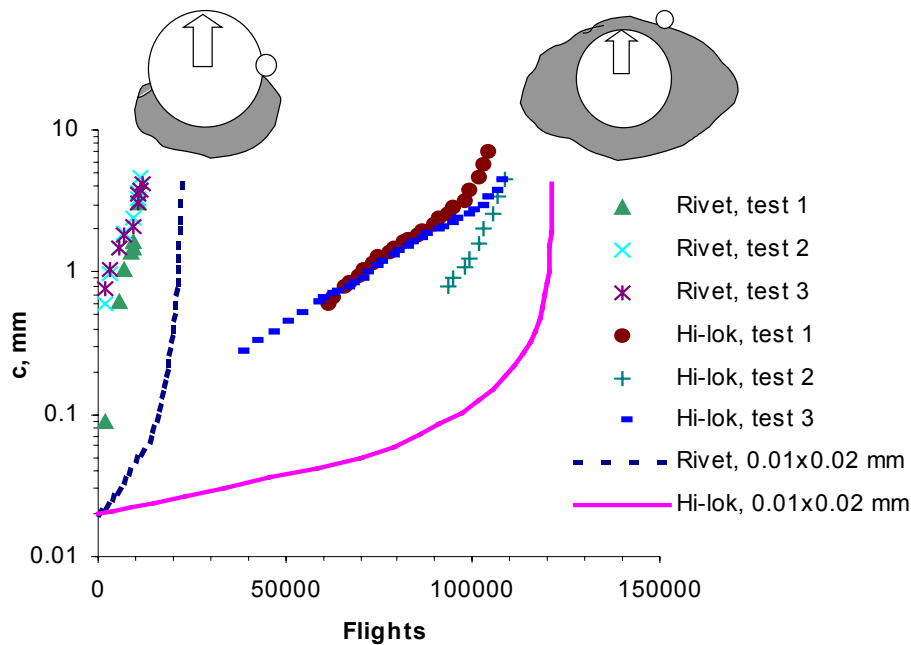


Fig.11: Comparison of fatigue crack growth for $\frac{1}{2}$ dogbone specimens with rivet fasteners and Hi-Lok fasteners.

Using the shakedown stress results of the $\frac{1}{2}$ dogbone specimens, the fatigue crack propagation was analysed according exactly to the same method as that used for the analyses of MSD panels. The predicted crack growths are shown in Fig.11 as a dashed curve for the rivet fasteners, and a solid curve for the Hi-lok fasteners. There is a reasonable agreement between predictions and test results for fatigue lives. The predictions are within a factor of two compared to the tests, indicating that the same analytical method is capable of dealing with the crack growth problems for significantly different joints and fastener systems. The large difference between predictions and test results of the crack growth for small crack sizes may be due to the reading threshold in the fractographic fatigue crack growth measurements when the crack size is small.

Multiple Site Fatigue Crack Initiation

A large number of similarly loaded fasteners will create a potential danger of multiple site crack initiation, such as those located at the centre part of the MSD panel as shown in Fig.1. This is an important issue for lightweight structures since the structural optimisation may lead to similar stress for many fasteners. The fact that fatigue cracks are often initiated inside of the joints makes the inspection of crack very difficult. Apparently, it is not reasonable to assume crack initiation occurring simultaneously at all the possible critical locations. A defect may or may not grow at a critical location due to variations in the size of defect, local material property, and stress etc. A probabilistic evaluation of how many cracks may be initiated will provide a much more realistic information about fatigue strength of the fastener joints.

A good probabilistic analysis should be based on reliable deterministic analyses. Since the non-linear finite element analyses and the advanced crack growth model provide a reasonable estimation of crack initiation and propagation for various types of joints and fastener systems, they provide a good basic platform for the probabilistic analysis of multiple crack initiation.

In the probabilistic analyses, the first problem is to determine whether or not an initial defect may be developed into a fatigue crack. Under constant amplitude fatigue loading, a crack growth threshold is often observed depending on the stress ratio and environment. The threshold is a complicated value when the spectrum loading is involved. Recent developments indicate that an “intrinsic” threshold²⁰ may be found for a given material if the crack closure is considered. The intrinsic stress intensity factor is less dependent on stress ratio or load so that it may be used to deal with the crack initiation under a spectrum loading condition.

Assuming all the initial defects can act as initial cracks, a state function may be defined according to the effective stress intensity factor range and the intrinsic threshold value:

$$g_T = \Delta K_T - \Delta S_{eff} Y(a_{th}) \sqrt{\pi a_{th}}, \quad (10)$$

where ΔK_T is the intrinsic threshold, ΔS_{eff} is an effective stress range, Y is a geometry function, and a_{th} is the crack size at which the effective stress intensity factor range reaches its minimum value.

The probability of crack initiation (POCI) is determined using the state function of eq. (10) for the probability of all $g_T < 0$ which determines the crack growth driving force being larger than the threshold value. Here, ΔS_{eff} represents the external load variation. Y represents the production variation, and a_{th} is a crack size which may be larger than the initial flaw.

According to level II²¹ analysis, a reliability index β_T is computed for POCI as:

$$\beta_T = \frac{\mu_{g_T}}{\sigma_{g_T}}. \quad (11)$$

This index is a ratio relating the mean and the standard deviation of the state function g_T . If g_T can be assumed as a normal distribution, β_T can be used to determine POCI according to:

$$POCI = \Phi(-\beta_T). \quad (12)$$

According to the state function, the mean value of g_T can be computed as:

$$\mu_{g_T} = E\{\Delta K_T - \Delta S_{eff} Y(a_{th}) \sqrt{\pi a_{th}}\} = \Delta \bar{K}_T - (\Delta K_{eff})_{\min} \quad (13)$$

where $\Delta \bar{K}_T$ is the mean intrinsic threshold. The stress intensity factor is determined by:

$$(\Delta K_{eff})_{\min} = E\{\Delta S_{eff} Y(a_{th}) \sqrt{\pi a_{th}}\}, \quad (14)$$

where $(\Delta K_{eff})_{\min}$ is the minimum effective stress intensity factor in the crack propagation analysis.

Suppose random variables ΔK_T , ΔS_{eff} , Y , and a_{th} are independent, the standard deviation of g_T can be calculated according to:

$$(\sigma_{g_T})^2 = Var\{\Delta K_T\} + Var\{\Delta S_{eff} Y \sqrt{\pi a_{th}}\}. \quad (15)$$

Here

$$Var\{\Delta S_{eff} Y \sqrt{\pi a_{th}}\} \approx v_K^2 (\Delta K_{eff})_{\min}^2 \quad (16)$$

where

$$v_K^2 = 0.25v_{a_{th}}^2 + v_Y^2 + v_S^2 + v_Y^2 v_S^2 + 0.25v_{a_{th}}^2 (v_Y^2 + v_S^2 + v_Y^2 v_S^2). \quad (17)$$

In this relation, v_S and v_Y are COVs of ΔS_{eff} and Y , and $v_{a_{th}}$ is the COV of a_{th} . The reliability index of POCI is determined by:

$$\beta_T = \frac{1 - (\Delta K_{eff})_{\min} / \Delta \bar{K}_T}{\sqrt{v_T^2 + v_K^2 [(\Delta K_{eff})_{\min} / \Delta \bar{K}_T]^2}} \quad (18)$$

where v_T is the COV of ΔK_T , and $v_{a_{th}}$ may be assumed to be the same as the COV of initial flaws.

To evaluate POCI, all the initial flaws are assumed to be able to propagate with different probabilities. A deterministic crack closure analysis is performed for the crack starting at the mean initial flaw. The minimum value of the effective stress intensity factor is determined during the crack growth analysis. Together with random values of threshold, geometry, stress, and crack size, the probability of crack initiation is determined.

When the probability of multiple crack initiation is determined, the probability of crack distribution for a given service time should be evaluated based on the distribution of initial defects and the stochastic crack propagation, see the upper right figure in Fig.12. To evaluate

the stochastic fatigue crack propagation once a crack starts to grow, a random form of Elber's crack growth rate, eq.(4), is considered (Wang, ref. 22)

$$\frac{da}{dN} w(K_{\max}) = X_i C_i (\Delta K_{eff})^{b_i}, \quad (19)$$

where C_i and b_i are determined by the mean crack growth rate. X_i is a probabilistic function used to characterise the stochastic crack growth due to material variation, see the right lower figure in Fig.12. To consider a full range fatigue crack growth rate, a piece-wise log-log linear approximation may be made in the crack growth rate so that not only mean values of C_i and b_i , but also the stochastic process X_i may be defined for various regimes in the fatigue crack growth rate.

When S_{\max} , the crack opening stress S_{op} , and the geometry function are treated as random variables to account for variations in the applied load, the crack closure, the geometry, and the crack configuration etc., the crack growth driving force ΔK_{eff} in eq.(19) becomes a random variable. Its statistical description may be approximated as:

$$\Delta K_{eff} = Z_{s_{eff}} \bar{S}_{eff} [Z_Y \bar{Y}(a)] \sqrt{\pi a} \quad (20)$$

The bars above variables represent mean values, and $Z_{s_{eff}}$ and Z_Y are normalised random variables representing randomness in stress and geometry. As the crack closure is directly affected by the applied load, a further simplification may be made by assuming a log normal variation in the applied load being in the same order as the log normal variation in the crack closure so that eq. (20) is replaced by

$$\Delta K_{eff} = \exp(z_S + z_Y) \overline{\Delta K}_{eff} \quad (21)$$

where z_S and z_Y are symmetrical random variables which can be approximated as normal distributions. They represent variations due to stress and geometry. When a piece-wise linear approximation is used for the mean crack growth data, the fatigue crack growth rate is determined according to

$$\frac{da}{dN} w(K_{\max}) = Z_i C_i [\overline{\Delta K}_{eff}]^{b_i} \quad (22)$$

where

$$Z_i = X_i \exp[b_i (z_S + z_Y)] \quad (23)$$

This model includes not only the variation in material property, but also variations in both load and geometry.

The exact stochastic solution of crack propagation is not straight forward for spectrum loading since one fatigue cycle may be followed by another cycle in a different regime. The cycle-by-cycle evaluation based on the crack closure model provides another solution since fatigue cycles or the part of fatigue cycles may be separated for those that affect the crack growth and

those that do not contribute to the crack growth. It is possible to extend the basic ideal of the Palmgren²³-Miner²⁴'s linear accumulative damage model, which is used widely in the S-N solutions, into a model to solve the non-stationary stochastic crack propagation (Wang, ref.23).

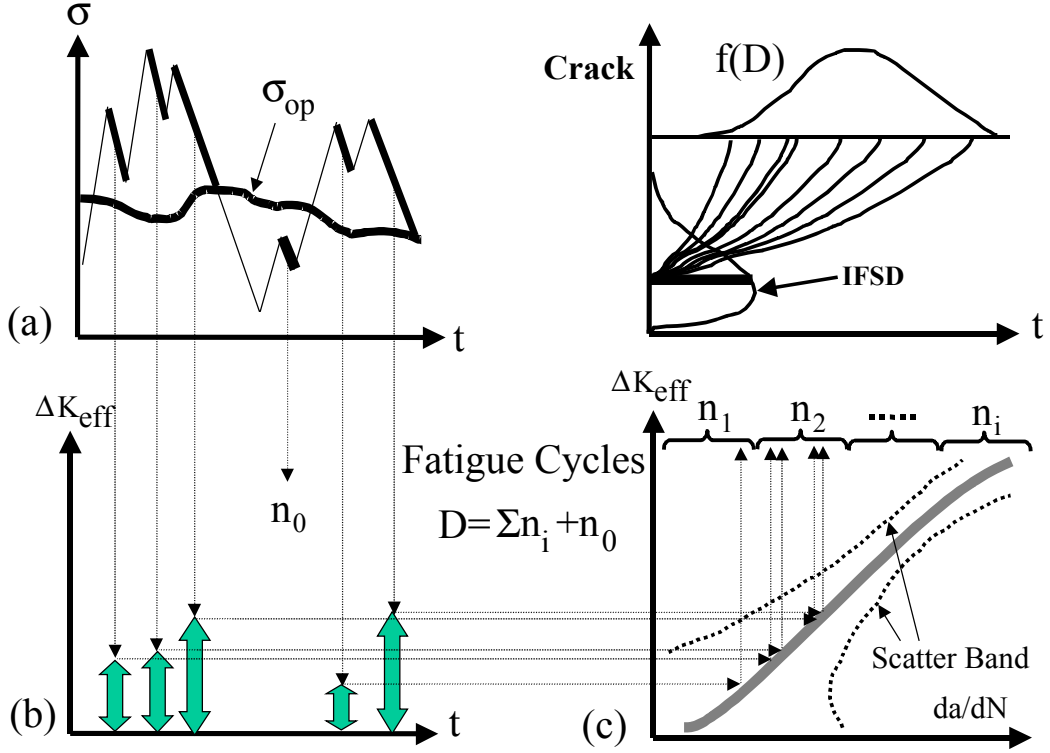


Fig.12: Schematic of the probabilistic fatigue crack growth model.

A simple schematic of the probabilistic damage accumulative model is shown in Fig.12. In this model, a deterministic cycle-by-cycle crack closure analysis is performed. The effective part of load cycle is computed following the thick lines as shown in Fig.12 (a). In this solution, the effective stress range is determined by:

$$\Delta S_{eff} = \begin{cases} S_{max} - S_{min} & \text{if } S_{min} \geq S_{op} \\ S_{max} - S_{op} & \text{if } S_{min} < S_{op} \\ 0 & \text{if } S_{max} \leq S_{op} \end{cases}, \quad (24)$$

where S_{op} is the crack opening stress. In this relation, the effective stress range is a mean value. It can be used together with the mean crack size to determined an effective stress intensity factor ΔK_{eff} as shown in Fig.12 (b) according to:

$$\Delta K_{eff} = \Delta S_{eff} Y(a) \sqrt{\pi a} \quad (25)$$

The mean crack growth rate is determined according to the intrinsic crack growth rate when ΔK_{eff} is determined as shown in Fig.12 (c). The effective stress intensity factor determines not only the mean crack growth rate, but also the stochastic crack growth regime for each load cycle.

Unlike the Palmgren-Miner's model, the damage parameter D is defined by the part of load cycles that actually contribute to crack growth. The damage parameter D , in the number of load cycles, is computed from a cycle-by-cycle evaluation of the crack growth for a given spectrum following the procedure as shown in Fig.12. D is determined as a sum of :

$$D = \sum_{i=1}^M n_i [(\Delta K_{eff})_i] + n_0 \quad (26)$$

where n_0 are the number of cycles with the stress range below the crack opening stress. Clearly, n_0 do not contribute to fatigue crack growth as shown in Fig.12 (b). The load cycles $n_i [(\Delta K_{eff})_i]$ are a sum of the cycles within a regime determined by $(\Delta K_{eff})_i$. Notice that, instead of using the rain flow counting method, $n_i [(\Delta K_{eff})_i]$ in eq. (26) are the load cycles defined by their effective stress intensity factors. Unlike the linear accumulation model in which the load cycles are not necessarily related to the crack growth, $n_i [(\Delta K_{eff})_i]$ depends on the crack size, the geometry, and the load and load history.

If the fatigue life is used to divide D as given in eq.(26), the damage parameter will be the same as that of the Palmgren-Miner's model for constant amplitude loading since the crack closure is nearly constant. For spectrum loading, the model is different since the damage accumulation is determined by the effective stress intensity factor that is a non-linear function of the crack size and load cycles. This model accounts for the load interaction effect, the stress state effect, as well as the small crack effect etc.

Yang and Manning²⁵ have developed a solution for a fully correlated non-stationary stochastic crack growth crossing several stochastic regimes. Their method can be modified to account for the non-stationary fatigue crack propagation in the damage accumulation model. According to Yang-Manning's model, the number of load cycles in each stochastic regime is recorded. A random variable is used to approximate the stochastic crack growth in each regime according to the crack growth rate as given in eq. (19). For each regime, the load cycles is approximated based on the stochastic crack growth rate derived from eq.(22):

$$n_i = \int \frac{w(K_{max}) da}{Z_i C_i [\Delta \bar{K}_{eff}]^{b_i}} = \frac{1}{Z_i} \sum \frac{w(K_{max}) \Delta a}{Z_i C_i [\Delta \bar{K}_{eff}]^{b_i}} = \frac{\bar{n}_i}{Z_i} \quad (27)$$

with the bar above n_i representing the mean value, and random variable Z_i determined by eq.(23). The total number of fatigue cycles, the damage parameter $D(a)$, is solved by

$$D(a) = \sum_{i=1}^m \bar{n}_i / Z_i + n_0 / Z_0 \quad (28)$$

where n_0 is the number of load cycles below the crack opening stress. n_0 doesn't contribute to the fatigue crack growth. It can be treated separately as a random variable.

In general, the log normal distribution is a good approximation for the base-line crack growth rate. When random variables Z_i are assumed to have a log normal distribution, it may be approximated in a distribution function of:

$$F_{Y_i}(x) = \Phi[\ln(x/M_i)/\sigma_i] = \Phi[\ln(x/M_i)^{1/\sigma_i}] = \Phi[\ln y] \quad (29)$$

Here, M_i is the 50% probability of the random variable Z_i . A substitution may be made for:

$$Z_i = M_i y^{\sigma_i} \quad (30)$$

where σ_i is the log normal standard deviation of Z_i . When the random variable y is considered to be the same for all the crack growth regimes, a complete correlated solution is found for $D(a)$:

$$D(a) = \sum_{i=1}^m \bar{n}_i / (M_i y^{\sigma_i}) + n_0 / (M_0 y^{\sigma_0}) \quad (31)$$

The distribution of fatigue cycles is solved for the combined effect of geometry, load, and stochastic crack growth:

$$F_D(D) = \int_0^D f_{\log normal}[y(D)] d[y(D)] \quad (32)$$

where $f_{\log normal}$ is the density function of a log-normal distribution. $y(D)$ is the reverse function determined by eq.(31).

The density of $D(a)$ is determined according to eq. (32)

$$f_D(D) = f_{\log normal}[y(D)] |\partial[y(D)] / \partial D| \quad (33)$$

Numerical methods may be used to solve the reverse function of $y(D)$, and the distribution and density of $D(a)$.

When the distribution of initial cracks is considered, its effect may be included in the model using an initial flaw size distribution (IFSD, see Fig.12). The distribution of fatigue life is determined by:

$$F_D(D|a) = \int_0^{\infty} F_D(D|a, a_0) f_{IFSD}(a_0) da_0 \quad (34)$$

Any distribution may be defined for IFSD. For convenience, IFSD is usually approximated as a log normal distribution:

$$\phi(a_0) = \frac{1}{\sqrt{2\pi}\sigma_0 a_0} \exp\left\{-\frac{[\ln(a_0/l_0)]^2}{2\sigma_0^2}\right\} \quad (35)$$

This distribution is determined by a median value (50 percent probability) l_0 , and a deviation of σ_0 . They are computed from:

$$l_0 = E\{a_0\} / \sqrt{1 + v^2(a_0)}, \quad (36)$$

$$\sigma_0^2 = \ln[1 + v^2(a_0)], \quad (37)$$

where $v(a_0)$ is the coefficient of variance (COV) for initial cracks which are defined by:

$$v(a_0) = \sqrt{\text{Var}\{a_0\}} / E\{a_0\} \quad (38)$$

In applications, the distribution of crack size for a given service time may be needed. The distribution is determined from $D(a)$ since the even $\{x \leq a\}$ is the same as the even $\{n \geq n_f\}$.

The distribution function of crack size, the $F_{FSD}(a|n_f)$, is determined by:

$$F_{FSD}(a|n_f) = 1 - F_D(n_f|a) \quad (39)$$

where $F_D(n_f|a)$ is the probability of the damage cycles n_f for a given crack size a .

According to this model, MSD (Fig.13 (a)) test results are considered. The initial flaws are approximated using the scatter in metallurgical defects in aluminium alloys. According to the scanning electron measurements of the material from ref. 15, $COV_{a_0} = 0.8$ is considered to be reasonable to characterise the scatter in initial flaws. The parameters in the intrinsic crack growth rate, the X_i in eq.(19), are determined based on the evaluation of AGARD small crack growth test results (Newman and Edwards, ref.²⁶). COV_X in the crack growth rate is fitted as a function of the crack growth rate:

$$COV_X = \begin{cases} A(da/dN)^B & \text{for } da/dN \leq 5 \times 10^{-6} \text{ mm/cycle} \\ Const. & \text{otherwise} \end{cases} \quad (40)$$

Three values are needed to define COV_X ; one for COV_X at $5 \times 10^{-6} \text{ mm/cycle}$ (the long crack data), one for COV_X at 10^{-8} mm/cycle (near threshold value), and one for COV_X of fatigue cycles less than crack closure. Apparently, COV_X for the crack growth rate larger than $5 \times 10^{-6} \text{ mm/cycle}$ is approximated using the scatter in the long crack growth test data with a value of $COV_X = 0.1$.

The AGARD small crack tests indicate that a value of $COV_X = 1.8$ is required for the scatter near the threshold regime, the crack growth rate close to 10^{-8} mm/cycle . This value gives the best overall coverage for all the scatters for both the constant and variable amplitude loading conditions in the AGARD small crack growth test results for 2024 T3 alloy.

The fatigue cycles below the crack closure have no effect on crack growth. However, since the crack closure is a stochastic process, it will affect the number of cycles below the closure. An empirical parameter is assumed to account for the variation in fatigue cycles below the

closure. According to the AGARD spectrum fatigue testing results, COV_X is found to be close to 0.1.

Under a laboratory condition, the load control can be assumed to be deterministic with $COV_S = 0$. Various values may be tried and compared to test results of MSD panels for COV_Y since there is no pre-knowledge existed. It has been found that $COV_Y = 0.2$ gives excellent results compared to the test results for 11 MSD test panels. The comparison is shown in Fig.13 (c) for the load level of 100 MPa. In this figure, POCB is the probability of crack breaking-through defined by the probability of cracks to penetration the sheet at a given time.

An extension of the analysis is to investigate the effect of load level on the onset of MSD. For different load levels, the analytical results are presented in Fig.13 (c). These analytical results showed that the load level has substantial effect on the POCB. High load will lead to a large POCB, a high percentage of MSD initiation, while reduction in the stress can significantly reduce the onset of MSD. The analytical results show that the log slope of multiple cracks is nearly independent of the load level, indicating that a constant ratio of MSD initiation may appear at various load levels for a given production consistency.

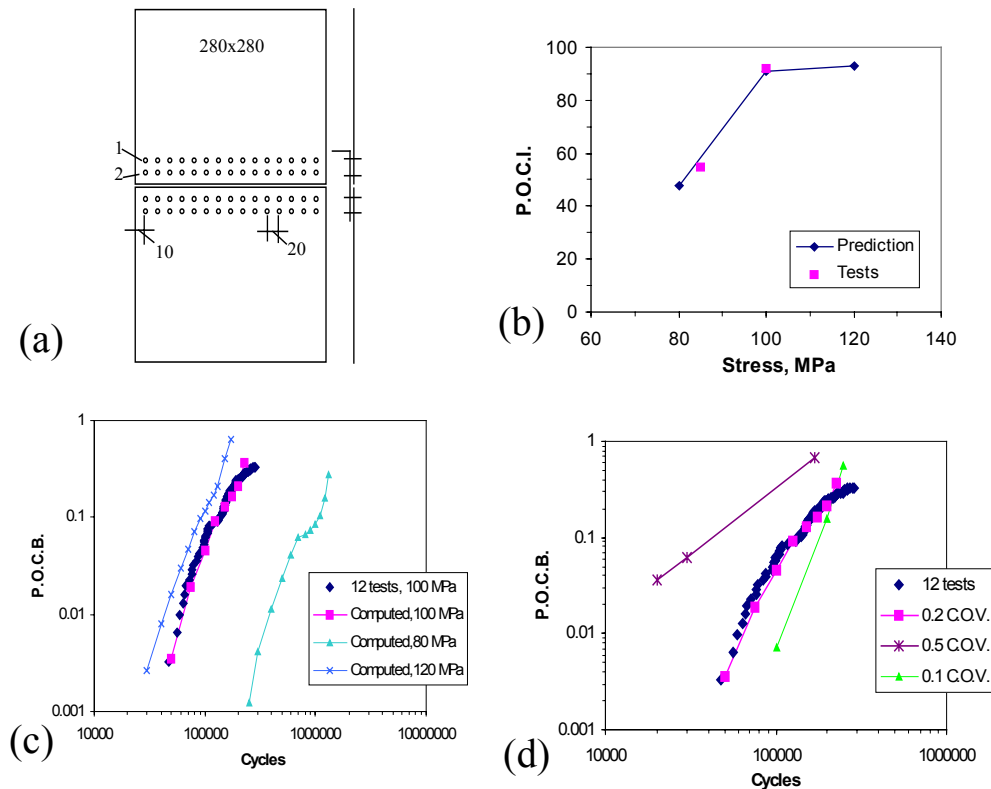


Fig.13: Probabilistic evaluation of the probability of crack initiation and the probability of breaking through cracks for the MSD panels.

According to the probabilistic solution, the effects of variations due to material, geometrical inconsistency, initial flaws, and load level may be separately considered. For example when

the production consistency is improved, resulting in a reduction in COV_Y from 0.2 to 0.1, the onset of MSD will be delayed, see Fig.13 (d). This will lead to an increased fatigue life for a given risk level even though the material and load are the same. However, the improvement increases the slope of POCB that will lead to a rapid build-up of multiple cracks within a relative short time span at the end of the fatigue life. This will create a more severe MSD situation at the later stage. MSD may appear “suddenly” everywhere after a certain service time, see Fig.13 (d).

On the other hand for a deteriorated production consistency, more cracks may be initiated at the early stage as the example shows in Fig.13 (d) when COV_Y has been changed from 0.2 to 0.5. The fatigue life will be reduced for a given reliability due to the early initiation of MSD. The development of MSD is more gradual, leaving significant damage indications before failure occurs since the slope of POCI is reduced.

Fractographic inspections of the broken MSD panels indicated there are a small number of locations that don't show any sign of crack initiation even under a stress level of 100 MPa. There is a correlation between the number of cracks and the load level. The trend shows that the higher the load, the more cracks may be founded in the broken specimens. The analytical results of POCI according to eq.(10-18) are shown in Fig.13 (b) for MSD panels compared to test results as a function of the load level. In this evaluation, scatters in the intrinsic threshold and the production consistency etc., are considered. The computed POCI's is denoted as “Computed”. The analytical results show a rapid drop in POCI when the stress level is reduced, indicating that MSD may not be a serious problem for low load level. For the load level where test results are available, the analytical results agree very well with the experimental results.

Environmental Impact

Even though the probabilistic analyses provide important information about the initiation and state of the MSD, a concern remains about how the fatigue may behave under the service condition where environmental attacks may occur. The contact analyses of MSD panels show that a substantial area around the fastener hole is free from contact for the rivet fasteners. When such joint is subjected to environmental attacks, these areas may trap harmful chemical elements and environmental assisted crack initiation and propagation could occur.

Environmental attacks leads to many consequences, such as the loss of thickness, pillowing²⁷, and pitting²⁸ etc.. While the loss of thickness and pillowing may increase stress severity, the pitting leads to initiation of fatigue cracks. Once a crack is initiated, the environment may speed up the crack growth rate. There are extensive investigations for the pitting growth in aluminium alloys. For example in the aquatic environment, the pitting growth on the surface of an aluminium plate may be approximated (ref.^{29 30}) with an empirical relation of

$$a = Pt^{1/3} + a_0 \quad (41)$$

where a_0 may be characterised with inclusions, particles, or machine scratches (the physical initial flaws), and P is a parameter used to characterise the pitting rate.

The pit growth is usually in proportion to the material volume so that the growth rate may be reduced when the pit becomes large. According to the pitting model by Harlow and Wei (ref.³¹), the pitting can significantly affect the fatigue life of the MSD panels especially in the early stage of crack initiation.

A competition model may be used to establish a relation between the pitting growth and the fatigue crack growth model³² because pitting controls the damage growth until corrosion fatigue crack growth dominates, transition from pitting to corrosion fatigue is dictated by:

$$\Delta K_{eff} \geq \Delta K_T \quad (42)$$

When the effective stress intensity factor is larger than the threshold ΔK_T , a competition may be considered between the pitting growth rate and the fatigue crack growth rate. The transition from the pitting growth mechanism to the fatigue crack growth mechanism may be determined by:

$$\left(\frac{dc}{dt}\right)_{fatigue} \geq \left(\frac{dc}{dt}\right)_{pitting} \quad (43)$$

This relation accounts for the load frequency effect. For example, when the load frequency is high, early transition may occur from the pitting mechanism to the fatigue propagation mechanism. The low load frequency may delay the transition from pitting to fatigue crack propagation.

Suppose that an average environmentally assisted crack growth acceleration may lead to about three times (according to ref. ³³) faster in the baseline crack growth rate, the fatigue life may be simulated with the pitting and competition model for the MSD panels for different usage frequency. Fig.14 (a) shows the analytical mean S-N curves for the MSD panels when environmental attacks are considered. For a 100 MPa load level for example, the simulations show that environmental attacks reduce the break-through fatigue life from the original 100,000 cycles to around 10,000 cycles for a load frequency of ten cycles every day. The fatigue cycles may be reduced even more, down to 5,000 cycles, for a frequency of usage down to once every two days. The environmental effect is especially significant when long fatigue lives are considered at the low usage frequency. There is an increasingly rapid reduction in the fatigue life for low stresses.

Monte-Carlo simulations were made for different initial flaw sizes, threshold values, pitting growth rates, and the stochastic crack growth rate etc. In such a simulation, a random initial crack size is chosen, a random crack growth threshold is determined, and the pitting damage and fatigue crack growth are evaluated. Based on the competition model, a sample crack growth is calculated. Repeat simulations can provide a distribution of damage for a given service time. In this way, the crack growth in a MSD panel is analysed. Fig.14 (b) shows several simulations with or without environmental effect. The simulations show that environmental attacks can significantly affect the probabilistic fatigue crack growth (up to an order of magnitude in fatigue life).

To provide a complete picture of the MSD scenario under the effect of environmental attacks, the probability of crack breaking-through (POCB) is again considered. Fig. 14 (c) shows an example of simulated POCBs for different scenarios. For example when there are no environmental attacks, there is only one out of 1000 holes may have a through-the-thickness fatigue crack for a stress level of 100 MPa at a service time of nearly 10 years with a usage frequency of 10 flights every day. When there are environmental attacks at every holes (100 % corrosion), there may be 76 out of 100 locations having cracks being grown through the thickness. This is a severe MSD scenario since all the holes may contain at least one crack.

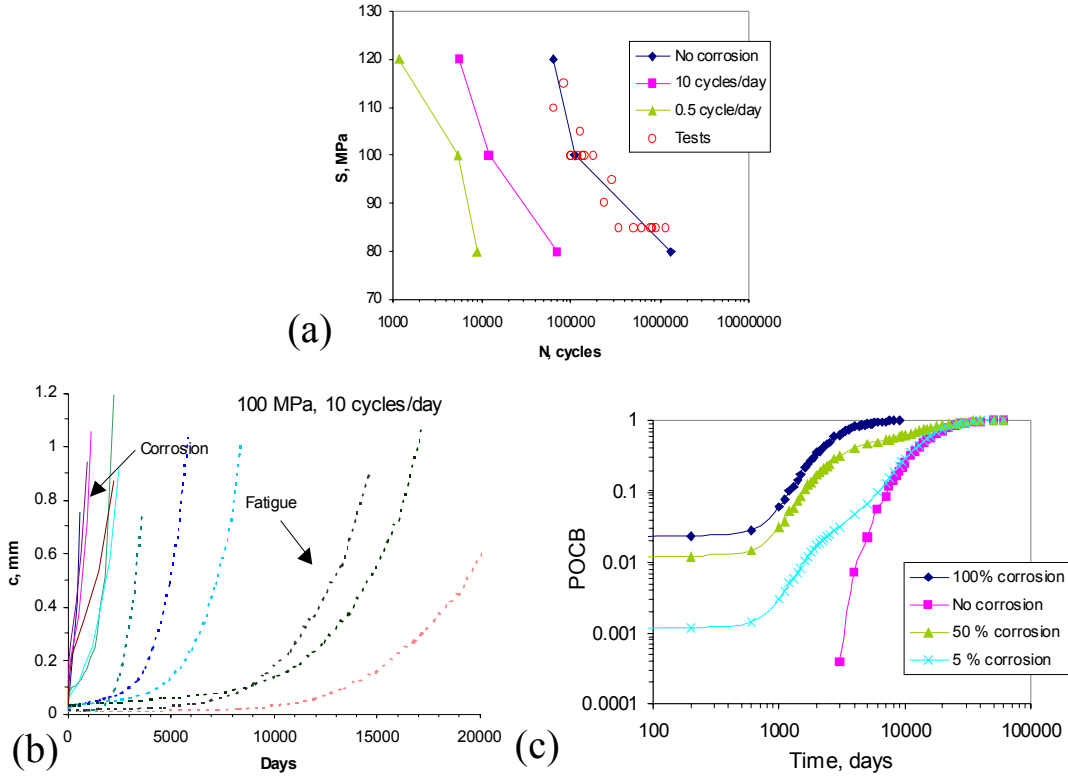


Fig.14: Effect of environmental attacks on the onset of MSD.

For practical applications, the scenario may be between these two extremes. When both fatigue and corrosion mechanism are involved, the POCB can be estimated according to:

$$POCB = POCB_{corrosion} \times POEA + POCB_{fatigue} \times (1 - POEA) \quad (44)$$

where $POEA$ stands for the probability of environmental attacks, which represent the percentage of the locations exposed to environmental attacks. $POCB_{corrosion}$ is the probability of crack growth due to the corrosion assisted mechanism, and $POCB_{fatigue}$ is the probability of crack growth due to only the fatigue mechanism.

Some cases are shown in Fig.14 (c) for different extent of environmental attacks. For example when 50% of holes are subjected to environmental attacks ($POEA = 0.5$), there will be 37 out of 100 locations where cracks may break through the thickness during 10 years service time for 10 cycles per day. This value is much lower than that when all the holes have been subjected to environmental attack (76 out of 100). If $POEA$ can be reduced to 5 %, the probability of crack breaking through the thickness (POCB) will be reduced to be less than 5 out of 100 during 10 years service. In this case, there is less chance that MSD may lead to a seriously problem.

The simulation indicates that environmental attacks have significant effect on MSD initiation and propagation, especially when $POEA$ is high. This often leads to problems that fatigue

cracks may be initiated at locations where they are not supposed to be (for example away from the sides of hole for rivet fasteners). The full scenario should be analysed both for the stress severe and corrosion severe areas. Together with stress and crack growth analyses, various scenarios may be analysed and compared to each other to find the most unfavourable combination.

Concluding Remarks

Finite element analyses involving friction, contact, non-linear material and geometry effect etc., were performed to identify stress behaviour around mechanical fasteners. It has been shown that it is necessary to make elastic-plastic and geometrical non-linearity analyses in addition to friction and contact in order to determine stresses around mechanical fasteners. The modern finite element codes can be used to identify fatigue critical locations even for the advanced fastener systems.

Under fatigue loading, the finite element analyses revealed that a shakedown condition exists at both low and high load due to friction, interference fitting, clamping force, and plastic yield. The shakedown creates a less fatigue severe state that explains why mechanical fasteners often have better fatigue lives than they are supposed to be. It has been found that reasonably accurate analyses may be performed according to the superposition principle of linear elasticity based on the shakedown condition. Together with an advanced crack closure model, fatigue lives may be analysed with limited test verifications for various types of joints and fastener systems even when variable amplitude fatigue loading is considered.

Since the deterministic fatigue life can be analysed with reasonable accuracy, it is meaningful to consider the stochastic fatigue crack propagation and scatters in initial flaws, material, production consistency, and fatigue loading. The significance of such analyses is that the multiple site fatigue damage scenarios may be determined, and effect of environmental attacks may be analysed. The analyses provide valuable information for the design of new joint systems as well as the evaluation of ageing structures.

Acknowledgement

Financial support from the Swedish Defence Material Administration, and the internal founding of Aeronautics Division, the Swedish Defence Research Agency, is gratefully acknowledged for the investigation.

References

¹ Gattaneo, G., Gavallini, G., and Galatolo, R., "Structural Maintenance of Aging Aircraft: Experiments on W.F.D.," *Doc. No. SMAAC-TR3.2-07-1.3/AEM, BRITE-EURAM, Proj. No. BE95-1053*, Contract No. BRPR-CT 95-0079, Dept. of Aerospace Engineering, Univ. of Pisa, Italy, June, 1998, 155p.

² Hibbit, Karlsson & Sorensen, Inc., "ABAQUS/Standard user's manual," 1998, Volume II, Version 5.7.

³ Elber, W., "Fatigue crack closure under cyclic tension," *Engng. Fracture Mech.* Vol. **2**, No.1, 1970, pp.37-45

⁴ Dugdale, D.S., "Yielding of steel sheets containing slits," *J. of Mech. and Phy. of Solids.* Vol.**8**, No.2, 1960, pp.100-104

⁵ Barenblatt, G.I., "The mathematical theory of equilibrium cracks in brittle fracture," *Advances in Applied Mechanics*, Vol.**7**, 1962, pp.55-129.

⁶ Wang, G. S., "The plasticity aspect of fatigue crack growth," *Engng. Fracture Mech.* Vol.**46**, No.6, 1993, pp.909-930.

⁷ Wang, G. S. and Blom, A. F., "A strip model for fatigue crack growth predictions under general load conditions," *Engng. Fracture Mech.* Vol.**40**, No.3, 1991, pp.507-533.

- ⁸ Dill, H.D. and Saff, C.R., "Spectrum crack growth prediction method based on crack surface displacement and contact analyses," American Society for Testing and Materials, *ASTM STP 595*, 1976, pp.306-319
- ⁹ Fuehring, H. and Seeger, T., "Dugdale crack closure analysis of fatigue cracks under constant amplitude loading," *Engng.Frac.Mech.* Vol.11, No.1, 1979, pp.99-122.
- ¹⁰ Newman, J.C., Jr., "Prediction of fatigue crack growth under variable-amplitude and spectrum loading using a closure model," American Society for Testing and Materials, *ASTM STP 761*, 1982, pp.255-277.
- ¹¹ Rice, J.R., "Some remarks on elastic crack tip stress fields," *Int.J.Solids Struct.* Vol. 8, No.6, 1972, p.751.
- ¹² Wang, G. S., "A generalised WF solution for mode I 2D part-elliptical cracks," *Engng. Frac. Mech.*, Vol.45, No.2, 1993, pp.177-208.
- ¹³ Wang, G. S., "A Strip Yield Analysis of Fatigue Crack Growth in the Residual Stress Field," *Int. J. of Fracture*, Vol. 96, No.3, 1999, pp.247-277.
- ¹⁴ Laz, P.J. and Hillberry, B.M., "Fatigue life prediction from inclusion initiated cracks," *Inter. J. Fatigue*, Vol. 20, No.4, 1998, pp. 263-270.
- ¹⁵ Wang, G. S., "Intrinsic statistical characteristics of fatigue crack growth rate," *Engng. Fracture Mech.* Vol. 51, No.5, 1995, pp.787-803.
- ¹⁶ Wang, G. S., "Post Yield Fatigue Crack Growth Analyses," *Engng. Frac. Mech.* Vol. 64, 1999, pp.1-21.
- ¹⁷ Waterhouse, R.B., "Fretting fatigue", *International Materials Reviews*, Vol. 37, No.2, 1992, pp.77-97.
- ¹⁸ Moesser, M., Elliott III, C.B., Kinyon, S., Flournoy, T., and Hoepfner, D. W., "The role of fretting corrosion and fretting fatigue in aircraft rivet hole cracking-status of an FAA program," *ICAF 95*, May 3-5, 1995 Melbourne, Australia, Vol. II, pp.1053-1068.
- ¹⁹ Hoepfner, D. W. And Goss, G. L., "A fretting fatigue damage threshold concept," *Wear*, Vol. 27, No.1, 1974, pp.61-70.
- ²⁰ Doecker, H. And Bachmann, V., "Determination of crack opening load by use of threshold behaviour," American Society for Testing and Materials, *ASTM STP 982*, 1988, pp.247-259.
- ²¹ Carpinteri, A., ed., "Handbook of Fatigue Crack Propagation in Metallic Structures," Elsevier Science, Amsterdam, 1994, p.1744.
- ²² Wang, G. S., "A Probabilistic Damage Accumulation Solution Based on Crack Closure Model", *Int. J. of Fatigue*. Vol.21, No.6, 1999, pp.531-547.
- ²³ Palmgren, A. L., "Endurance of ball bearings," *VDI Zeitschrift*, Vol.68, No.14, 1924, pp.339-341.
- ²⁴ Miner, M. A., "Cumulative Damage in Fatigue," *J. of Applied Mech.*, Vol.12, No.3, 1945, pp.159-164.
- ²⁵ Yang, J. N. And Manning, S. D., "Stochastic crack growth analysis methodologies for metallic structures," *Engng. Frac. Mech.*, Vol.37, No.5, 1990, pp.1105-1124.
- ²⁶ Newman, J. C., Jr., and Edwards, P. R., "Short-crack growth behaviour in an aluminium alloy-an AGARD cooperative test programme," R-732, AGARD, Dec. 1988.
- ²⁷ Komorowski, J. P., Bellinger, N. C., and Gould, R. W., "The role of corrosion pitting in NDI and in the structural integrity of fuselage joints", *ICAF 97: Fatigue in new and ageing aircraft*, vol. 1, R. Cook and P. Poole, eds (London: Engineering material advisory services Ltd., 1998), pp.251-266.
- ²⁸ Kitagawa, H., Fugita, T., and Miyazawa, K. "In Corrosion-Fatigue Technology," American Society for testing and Materials, *ASTM STP 642*, 1978, pp.98-117.
- ²⁹ Hoepfner, D. W., "Model for prediction of fatigue lives based upon a pitting corrosion fatigue process. Fatigue Mechanisms," American Society for Testing and Materials, *ASTM STP 675*, 1979, pp.841-870.
- ³⁰ Turnbull, A., "Review of modelling of pit propagation kinetics," *British Corrosion Journal*, Vol.28, No.4, 1993, pp.297-308.
- ³¹ Harlow, D. G. and Wei, R. P., "Probabilities of occurrence and detection of damage in airframe materials," *Fatigue Fract. Engng. Mater. Struct.*, Vol.22, 1999, pp.427-436.
- ³² Chen, G. S., Wan, K. -C., Gao, M., Wei, R. P., and Flournoy, T. H., "Transition from pitting to fatigue crack growth – modelling of corrosion fatigue crack nucleation in a 2024-T3 aluminium alloy," *Materials Science and Engineering A219*, 1996, pp.126-132.
- ³³ Wei, R. P. and Harlow, D. G., "Probabilities of occurrence and detection, and airworthiness assessment," *ICAF '99*, Bellevue, WA, U.S.A., July 14-16, 1999.